Available online at www.sciencedirect.com
SCIENCE DIRECT®
International Journal of Thermal Sciences 45 (2006) 269–283
International Journal of Thermal Sciences
www.elsevier.com/locate/ijts

A study of local heat transfer mechanisms along the entire boiling curve by means of microsensors

M. Buchholz [a], H. Auracher [a,*], T. Lüttich [b], W. Marquardt [b]

[a] *Institut für Energietechnik, Technische Universität Berlin, Marchstr. 18, KT1, D-10587 Berlin, Germany*
[b] *Lehrstuhl für Prozesstechnik, RWTH Aachen, Turmstr. 43, D-52064 Aachen, Germany*

Received 22 December 2003; received in revised form 24 August 2004; accepted 24 August 2004

Available online 12 October 2005

Abstract

An array of 36 microthermocouples (38 μm diameter) embedded in a horizontal copper heater (distance to the surface 3.6 μm), a micro optical probe (tip diameter ∼1.5 μm) and a microthermocouple probe (tip diameter ∼16 μm), both moveable above the heater surface, are applied to study heat transfer mechanisms along the entire boiling curve under steady-state conditions. Test fluids are isopropanol and FC-3284. In nucleate boiling, very localized and rapid temperature drops are observed indicating high heat fluxes at the bottom of the bubbles. Already before reaching CHF, hot spots occur the size of which increases towards the Leidenfrost point. In the entire transition boiling regime wetting events are observed, but no ones in film boiling. In low heat flux nucleate boiling small vapor superheats exist in the bubbles and strong superheats in the surrounding liquid. This characteristic changes continuously with increasing wall superheat: the liquid surrounding the vapor approaches saturation whereas the vapor becomes more and more superheated. In film boiling the bubbles leaving the vapor film can reach superheats of 40 K near the surface. The optical probes confirm a liquid rich layer near the surface between nucleate boiling and high heat flux transition boiling. The void fraction in this layer increases continuously with the distance to the surface until a maximum value which seems to be linked to the bubble departure diameter.

Keywords: Microthermocouple; Optical probe; Microthermocouple probe; Pool boiling; Transition boiling; Surface wetting; Dry patch; Surface temperature; Boiling mechanism; Void fraction; Isopropanol; FC-3284; PF-5052; Temperature field; Temperature control; Two phase flow

1. Introduction

In spite of the huge amount of studies on boiling heat transfer in the past, the number of investigations does not decrease, indicating that this complex process is still not well understood. Nevertheless significant progress has been achieved in recent years. This is because more sophisticated experimental techniques and data acquisition systems as well as significantly improved mathematical tools are now available. Hence, our ability to explore the basic mechanisms of boiling has been improved and those results are increasingly used to develop physically based heat transfer models. They are more generally valid than empirical correlations and, last but not least, a deeper knowledge of the governing physical mechanisms gives us the chance to develop enhanced heat transfer surfaces systematically and not by trial and error methods.

The governing mechanisms of boiling take place very near to the surface. If a thin electrically-heated plate is used as test heater, bubble and vapor spot dynamics at the surface can be studied nonintrusively by liquid crystals [1] or infrared-thermography on the rear surface. By means of liquid crystals it was possible to confirm qualitatively intensive evaporation in the micro region at the bottom of a bubble [2]. Furthermore, first attempts have been made recently to develop mechanistic models for nucleate boiling based on liquid–crystal data [3]. This study revealed that liquid crystal thermography has a limited temporal resolution. This shortcoming might be overcome by highspeed infrared thermography. But even though, validation of a boiling model also needs data on the two-phase characteristics above the surface, such as information about bubble growth, bubble coalescence etc. Moreover, real heating surfaces

* Corresponding author.
E-mail address: auracher@iet.tu-berlin.de (H. Auracher).

1290-0729/$ – see front matter
doi:10.1016/j.ijthermalsci.2004.08.007

Nomenclature

CHF	critical heat flux	P_t	roughness parameter according to DIN EN ISO 4287 ..... µm
EMF	electromotive force V	$\dot{q}$	heat flux ..... $W{\cdot}cm^{-2}$
G	gain, output voltage/input voltage	$\dot{q}^*$	dimensionless heat flux $\dot{q}/\dot{q}_{CHF}$
K_{pp}	peak-to-peak temperature fluctuations (noise) .. K	ΔT	heater surface superheat, $T_{surface} - T_{sat}$ ..... K
MOP	micro optical probe	ΔT_p	MTCP superheat, $T_{probe} - T_{sat}$ ..... K
MTC	microthermocouple	TC	thermocouple
MTCP	microthermocouple probe	z	distance perpendicular to the heater surface ..... mm or µm
p^*	reduced pressure, p/p_c	α_v	void fraction
PIF	phase indicator function		

are thick and the boiling mechanism may differ from the one on thin foils, see [4,5] for example. In particular, the temperature field dynamics in the heater body plays a role and should be taken into account. Hence, a complex three-dimensional multiphase flow problem connected to a three-dimensional heat conduction problem has to be tackled.

If thick heaters are to be studied as in the present report, nonintrusive temperature measurement techniques such as liquid crystals or thermography are not applicable. Other nonintrusive techniques for investigating the two-phase flow characteristics like high-speed video, x-ray attenuation etc. are of limited benefit because these methods cannot access the most important parameters determining two-phase flow in the region of high void fractions. Miniaturized sensors are preferred if they do not significantly disturb the processes taking place inside and above the heater. This was the focus of our studies in recent years. To enable measurements along the entire boiling curve, a temperature control system for steady-state experiments in the whole range between nucleate and film-boiling has been developed. Micro optical probes with sensitive tip diameters of less than 1.5 µm were used to study the two-phase behavior as a function of the distance to the surface [6,7]. Measurements of void fractions and contact frequencies down to very small distances to the surface (8 µm) were possible without significant distortion of the local flow. With a 4-tip probe, velocities and bubble sizes could also be estimated. The existence of a liquid rich zone above the heater surface was proved for the region between nucleate boiling and high heat flux transition boiling. A minimum void fraction occurs at the surface and a maximum at about half of the bubble departure diameter. The results suggest to modify the macrolayer theory [6]. The wetting behavior at the heater surface creates complex temperature fluctuations beneath the surface. Their characteristics in time and space depend on the properties of the heater material and have in turn an influence on the wetting dynamics. Microsensors are required to record those fluctuations with a sufficient resolution. A promising approach has been carried out by Buchholz et al. [8]. They developed microthermocouples (MTCs) of 38 µm diameter with the sensitive tip 3.6 µm beneath the surface. Using the measured data, first results on the wetting mechanisms in the different boiling regimes were found [6, 7].

The first part of the present report gives a short summary of the technique to measure entire boiling curves under steady-state conditions as well as of the results obtained so far with micro optical probes and microthermocouples. Then new results found with these miniaturized sensors are presented. Special emphasis is laid on results with a new microsensor developed in the meantime, a needle-shaped microthermocouple probe (MTCP) with a diameter of about 16 µm at the tip. The junction is located about 1 µm above its tip. This probe enables measurements of vapor and liquid temperature fluctuations down to very small distances to the heater surface—a minimum distance of 10 µm has been realized so far. Measurements of local fluid temperatures using a combined probe consisting of a MTCP and a micro optical probe (MOP) are also presented. To account for the influence of fluid properties the experiments are carried out with two different fluids; isopropanol and the fluorinert FC-3284 (3M-company). The study has been carried out in close cooperation between the group at RWTH-Aachen which is focused on theoretical aspects and the one at TU-Berlin where the experimental work has been carried out [6].

2. Experimental facilities

2.1. Test loop and test heater

Test loop and test heater are described in detail in [6]. The pool boiling test loop is completely made of stainless steel, pickled, electropolished and passivated. Hence, tests with very clean liquids are possible. The maximum operation pressure is 1.0 MPa. The test heater is horizontally positioned in a test vessel. On its top, MOP or MTCP probes are installed. They are 3D-moveable above the heater surface by a micrometer and a piezo-electric adjusting device. The heater is made of copper with 35 mm diameter and 7 mm thickness. To prevent corrosion and oxidation, the boiling surface is coated with a pure gold layer of 1 µm thickness. Heat input is provided by a resistance heating foil which is pressed to the bottom of the heater. An upper limit of 5.5 $MW{\cdot}m^{-2}$ heat flux can be established.

2.2. Control concept

Local boiling phenomena along the entire boiling curve can only be studied in steady-state experiments. Therefore a tem-

perature controlling system is required to especially stabilize the transition boiling region. This is accomplished by a controller realized on a PC. The controller runs independently of the host PC processor on a signal processing card with an onboard DSP processor. The instantaneous average of 12 temperatures from thermocouples embedded below the heater surface is used as temperature input of the control loop. This temperature represents the average heater temperature. The total response time between a temperature change at the input and the response of the controller at the output is less than 1.5 ms. The output is amplified and supplied to the heating foil. A stability analysis revealed that even steep negative slopes of the boiling curve are accessible by this system [9].

2.3. Micro optical probes

To study two-phase parameters such as void fraction, contact frequencies, bubble sizes and velocities as a function of the distance to the heater surface, micro optical probes (MOP) are a very effective tool. Our probes [6,8] are made from a single mode quartz glass fiber with a cladding diameter of 125 μm and a core diameter of 8 μm. The tip of the probe is formed by etching in hydrofluoric acid. This method enables the preparation of very small probe tips. Measurements with a scanning electron microscope shows a tip diameter of less than 1.5 μm. The probe is 3D-moveable by means of micrometer stages. The position perpendicular to the test heater is measured both with the precision stage and a precision linear variable displacement transformer with an accuracy of ± 1.1 μm.

Four of these optical probes have been combined to form a 4-tip multiple probe. The optical fibers are placed next to each other (125 μm between each other in radial direction) with different axial distances. First experiments with the 4-tip probe have been published in [7,8]. In the present report we focus on more comprehensive data obtained only with the lowest tip of the probe. A stainless steel wire with 50 μm diameter is fixed to the probe ensemble with a radial distance of approx. 800 μm and at a given distance to the lowest probe tip. The wire is used for distance calibration purposes. The signals are sampled with an ADC-64 data acquisition board for PC hosting 32 differential input channels, 8 A/D converters each up to 200 kHz sampling rate at 16 Bit and an onboard DSP-processor (Innovative Integration Company). For the acquisition of the probe signals, 8 channels—which represents the minimum number of active channels—are used at full sampling rate (200 kHz per channel). All signals are sampled simultaneously. A 1-minute run at full 200 kHz generates about 200 MB binary data. Note, that only the lowest probe data is presented here.

2.4. Microthermocouples

Details of the design of the microthermocouples (MTC) have been presented in a previous report [8]. In the center of the test heater an array of 36 MTCs is implanted within an area of 1 mm^2. Each thermocouple consists of an insulated constantan thermocouple wire (38 μm diameter) which is embedded in the heater. The second conductor of the thermocouple is a sputtered copper layer (2.5 μm thick), contacted with insulated copper thermocouple wires. The copper layer is covered by a titanium layer of 0.1 μm thickness serving as diffusion barrier between the copper, and a final gold layer (1.0 μm thick), which protects the heater surface against corrosion. All layers are deposited by a DC-Magnetron sputtering process. The sensitive tips of the MTCs are located 3.6 μm below the surface. 8 additional MTCs with diameters of 50 μm each are placed around the MTC-array in the center to enable measurements of larger wetting structures. The surface of the heater has been prepared with emery paper up to grit P4000 before the final sputtering process with copper, titanium and gold. The latter do not change the mechanical features of the original surface as could be proved by 3-D surface topography measurements with a scanning stylus instrument [10].

Acquisition of temperature fluctuation signals is realized as follows. The copper layer is connected to a single reference junction kept at 0 °C via the copper wires. Each constantan thermocouple wire is connected to a very low noise instrumentation amplifier ($G = 700$). The output is filtered using a 4th order lowpass filter with a cutoff frequency of 7.5 kHz. The conditioned signals are sampled with two ADC-64 data acquisition boards for PC as described in Section 2.3. These data acquisition boards are installed in two separate PCs because of the large data streams. Groups of 8 channels are sampled simultaneously. A special software allows burst-mode operation to minimize the time lag between channel groups 1–8, 9–16, 17–24 and 25–32. At moderate sampling rates, MTC data can be assumed to be measured simultaneously. Both data ADC-64 cards are synchronized with a main data acquisition system by digital signals using two DaqBoard 2000 multifunction cards, each with 16 input channels at 16 Bit (IOtech company) installed in a third PC. A sampling rate of 25 kHz per MTC is used for the measurements.

2.5. Microthermocouple probe

The micro optical probes (MOPs, Section 2.3) enable the analysis of two-phase flow dynamics down to very small distances to the surface. However, they cannot detect temperatures in the two-phase layer. The development of a model for the boiling mechanism also requires information about the complex temperature field above the heater surface.

Several attempts have been made to study the temperature field in boiling processes by small thermocouples (TC). Jacob and Fritz [11] published measurements using a TC with wires of 0.2 mm diameter to determine steady-state temperature profiles in water above a heated surface. Later, Marcus and Dropkin [12] designed a stretched bare wire TC with one wire parallel to the surface, a wire diameter of 25.4 μm and a bead diameter less than 50.8 μm. They measured maximum, minimum and average temperatures above the heater during boiling of water. Wiebe and Judd [13] used a similar TC setup with a wire diameter of 25.4 μm and a bead diameter less than 76.2 μm. They measured mean temperature profiles in boiling R 113. Van Stralen and Sluyter [14] used a commercially available sheathed TC of 0.25 mm diameter to measure temperature fluctuations associ-

ated with steam bubbles above a heated wire. Delhaye et al. [15] developed a bare wire TC with a wire diameter 20 μm, but not of the stretched form type in order to avoid bubble deflection at the horizontal wire. They performed a statistical analysis of the signals. Their test fluid was water. Ganic and Afgan [16] analyzed the temperature field near steam bubbles. They used a bare wire TC with 12 μm wire diameter but did not report the bead size which determines the thermal behavior. More recently, Beckman et al. [17] developed a fast response TC and reported measurements in flow boiling of R 113. They used a type E TC with a wire diameter of 20 μm and a bead diameter of about 60 μm with a junction shaped as a disk with a diameter of 80 μm and a thickness of 2.5 μm. They reported also on a new version of the TC, see [18] with an increased disk diameter of 100 μm and also an increased thickness of 4 μm.

All these temperature sensors have some drawbacks due to their construction and/or their dimensions. Standard temperature sensors such as sheathed TCs are too large and also too slow to enable local measurements with acceptable temporal and spatial resolution. Commercial fine wire TCs can provide more localized measurements and faster response times. Unfortunately, additional sources of error are introduced because of their mechanical construction. Such TCs usually consist of two separate wires, roughly parallel to each other and connected at the active junction by some technique. A phase change from the liquid to the vapor phase can cause a liquid film to fill the gap between the wires. As the surface temperature of this film can be assumed to be at saturation temperature, an error is introduced as long as the liquid film is present. Experiments with a high speed video camera using droplets impinging on such TCs in the authors' lab have validated this conjectured effect. Consequently, the sensor should exclude this kind of effect by using a stretched setup or *one* wire instead of two. The stretched type on the other hand is not considered here, as bubbles "tend to avoid the hot junction by rolling around the (horizontal) wire" [19]. Thus, the TC should have a needle shape.

The construction of such an *one* wire TC means that deposition techniques need to be used in order to create the second conductor of the TC. For a fast response time of the TC, a thin wire is desirable. Flattening of the junction by any means [17, 18] is not considered to be useful as the size of the junction is greatly increased. Consequently local measurements—especially very close to the wall—are no longer possible.

Our microthermocouple probe (MTCP) is designed according to the considerations above (Fig. 1). A thin insulated constantan TC wire with a conductor diameter of 12.7 μm and a polyimide isolation thickness of 1.3 μm is connected to a constantan wire with a diameter of 50 μm (Fig. 2) in order to provide low electric resistance as this reduces electrical noise later during the measurements. A thin bare gold wire is placed about 2 mm behind the end of the thin wire and fixed with very little high temperature adhesive. In the next step a thin pure gold layer is added by vapor deposition to connect the gold wire and the cross-sectional area of the constantan wire at the tip of the MTCP. Afterwards, electroplating is used to increase the thickness of the gold layer. The thickness of the gold layer at the junction is estimated to be about 1 μm. The location of the junction is therefore known with high precision. The characteristics of a gold-constantan TC is very close to a standard type T (copper-constantan) TC. It enables the use of standard components for reference junction and cabling. Details are given in the following paragraph.

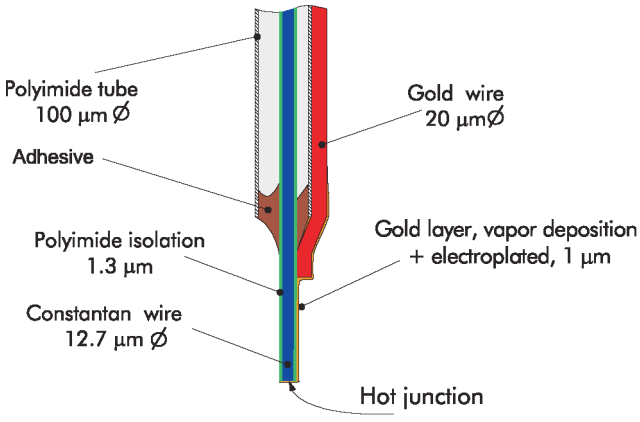

Fig. 1. Setup of microthermocouple probe.

Inside the probe support tube (see Fig. 2), the gold wire is connected to a copper TC wire in order to enable usage of standard TC wires of type T and also a standard type T reference junction. The gold-copper connection introduces an additional gold-copper thermocouple in the electrical loop which can affect measurement accuracy although the relative EMF of copper and gold are quite similar.

In order to access the potentially resulting measurement error, the characteristics of this material combination were investigated. For this purpose, a gold-copper TC was placed in a constant temperature calibration bath and connected with a gold-copper reference TC kept at 0 °C. Measurements were carried out between 20 °C and 140 °C. Not surprisingly, the measured output voltage is less than 1% of the standard type T TC throughout the entire temperature range. For our purposes, this error does not result in a relevant measurement error, because the gold-copper junction is located inside the probe support tube (6 mm diameter, see Fig. 2). There, the temperature corresponds to the fluid saturation temperature. It is fairly constant, since fluctuations possibly induced by the boiling two-phase flow are damped out due to relatively large tube mass and the thermal decoupling of the junction. Because of this construction, we get only a differential error as the constant TC voltage representing saturation temperature is still generated in the copper and constantan connection wires thus representing TC type T characteristics. The remaining error is compensated by a calibration curve which is deduced using the overall calibration curve and the gold-copper calibration curve.

The standard 63% response time $\tau_{63,\mathrm{MTCP}}$ of the MTCP was investigated prior to the pool boiling experiments using droplet impingement experiments. For a test run, a free falling droplet (about 50 mm free travel) of about 1 mm diameter impinged on the probe. An analysis of both, the MTCP signal and high speed video frames were used to determine $\tau_{63,\mathrm{MTCP}}$. In the experiments, $\tau_{63,\mathrm{MTCP}}$ can only be determined for a gas to liquid phase change. Four fluids were tested. We found

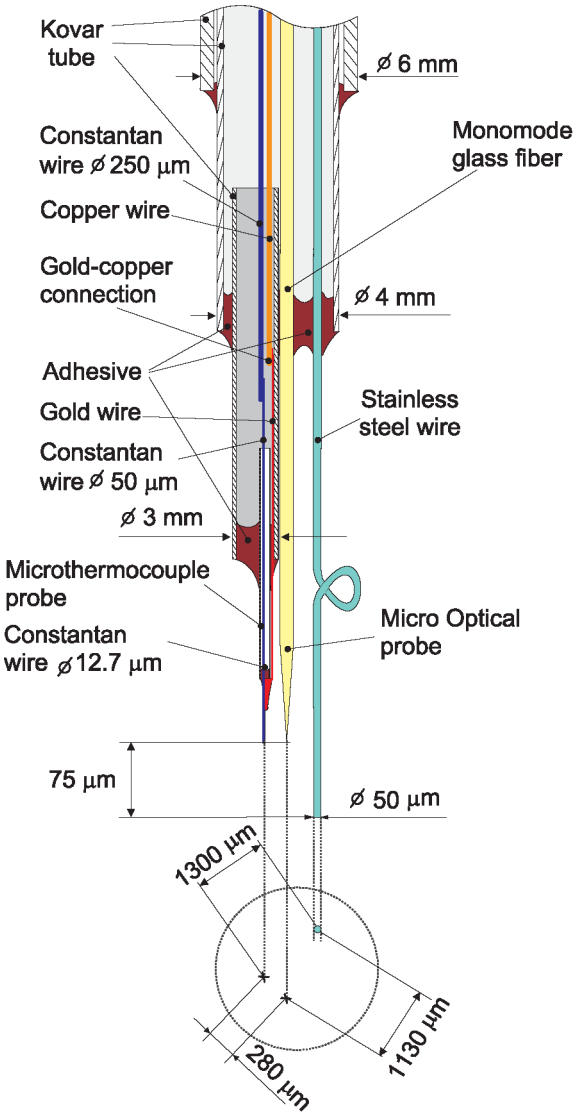

Fig. 2. Setup of combined MTCP-MOP probe.

response times of 0.15 ms for water, 0.24 ms for acetone, 0.27 ms for isopropanol and 0.36 ms for FC-72. However, the true $\tau_{63,\mathrm{MTCP}}$ values for the boiling experiments may deviate from these data, because the conditions—especially fluid velocity and level of turbulence—are expected to be different from those during the impingement experiments. Taking the highly agitated and turbulent two-phase layer above the surface into account, the response time maybe shorter during the boiling experiments.

The MTCP voltage is amplified using a special very low noise amplifier ($G = 700$). The signal is filtered with a 4th order lowpass with a cutoff frequency of 12.5 kHz. The signals are sampled with one ADC-64 card (see Section 2.3) at 200 kHz. This high sampling rate is not necessary for proper acquisition of the MTCP signals but is needed because of the simultaneous measurement of the signals of an optical probe which is located next to the MTCP (see next paragraph). The response time of the MOP is much faster than the MTCP thus a high sampling rate enables measurements with higher accuracy.

2.6. Combined microthermocouple and optical probe

For measurements in the two-phase layer above the heater, a combined probe consisting of a MTCP and a micro optical probe (MOP, see [6,7]) was manufactured. The schematic setup of the combined probe is depicted in Fig. 2. A stainless steel wire of a diameter of 50 µm with about 1 mm radial distance to the active probes is used for distance calibration purposes. The combination of both probe types is important for the interpretation of the MTCP probe signals. The state of phase at the MTCP tip cannot be derived directly from the temperature signal since we have little a priori knowledge on the temperature characteristics. Although the MOP is located with some radial distance from the MTCP to prevent liquid film buildup between MOP and MTCP, the simultaneously measured MOP data provides a valuable guidance for the interpretation of the measured temperature data and allows separation of liquid and vapor temperature.

3. Experimental procedure and data evaluation

3.1. Experimental conditions and procedure

Two sets of experiments are performed: one set using isopropanol and a second set using FC-3284 (identical with Fluid PF-5052, 3M Company) as test liquid. To guarantee a high purity of the test fluid, the entire amount necessary for the experiments is charged in vapor state and condensed inside the facility using the condenser on top of the boiling vessel (see [8]). The test liquid is thoroughly degassed prior to every experiment by vigorous boiling on the test heater as well as on tube coils inside the boiling vessel. The tube coils are heated to a high temperature during the degassing procedure. Throughout this procedure, inert gases are repeatedly removed at the top of the condenser using a vacuum pump. Afterwards, the temperature of the tube coils is reduced to a lower temperature slightly above saturation temperature of the test liquid.

A first set of experiments is performed with isopropanol at saturation conditions at a reduced pressure of $p^* = 0.022$ which corresponds to a pressure of 0.106 MPa and a saturation temperature of 83.3 °C. The last test series with the MTCP/MOP probe has been carried out at different conditions. Because of a defective temperature controller in the recirculated bath which sets the fluid temperature inside the boiling vessel, the fluid during this test series is slightly subcooled by about 0.5 K.

For the second set of experiments saturated FC-3284 is used as a test liquid, also at a pressure of 0.106 MPa. Unfortunately, the critical pressure of this fluid is not known, therefore we cannot report the reduced pressure. Some problems have also been encountered for the saturation temperature of this fluid. In the literature, a saturation temperature of 50.0 °C [20] at atmospheric pressure has been reported. Accurate measurements with thoroughly degassed FC-3284 [21] report a much higher saturation temperature of 53.2 °C at the same pressure. As can be expected from thermodynamics, a noteworthy volume fraction of inert gases should have a significant effect on the saturation temperature. In fact, FC-3284 can dissolve high volume

fractions of inert gases (54% [22]). Due to these problems for the evaluation of the experiments with FC-3284, we used the measured temperature inside the boiling vessel after the degassing procedure as saturation temperature as we believe this to be most appropriate and realistic. During evaluation of the saturation temperature, medium heat flux boiling was present both on the test heater and the tube coils inside the test heater.

All experiments are carried out at steady-state. To prepare for a test run, the heater temperature controller is set to a temperature for high heat flux transition boiling to activate possible nucleation sites in order to avoid hysteresis at boiling incipience. The heater temperature is afterwards set to the first point of a test run in nucleate boiling and the measurements are started after steady-state conditions of the test heater have been reached. Then the temperature is increased to the next set-point value etc. until heat transfer and MTC/MTCP/MOP-data at all desired heater temperatures have been measured along the entire boiling curve.

Three test series are presented in the present paper:

(1) measurements with MTCs along the entire boiling curve for both fluids (Section 4.2),
(2) measurements with MOP for both fluids, and
(3) measurements with the combined MTCP-MOP probe for isopropanol only.

Both probe experiment series cover a range of probe positions and some points of the boiling curve (Sections 4.3 and 4.4). For the MOP and MTCP-MOP test runs, data are taken for all different probe distances to the surface at a constant heater temperature. After the last measurement, the temperature setpoint is changed to the next value and again data for all selected probe distances are taken. The measurements are realized with stepwise increasing temperature between low superheat in nucleate boiling and high superheat in film boiling. Both the MOP and the combined MTCP-MOP are located above the center of the heater.

3.2. Data evaluation

Here, only data evaluation for the MTC and MTCP probe signals is discussed. Detailed information on the evaluation of boiling curves as well as on the identification of the phase indicator function (PIF) from MOP signals can be found in [8].

Due to improvements of the data acquisition system for the MTCs, no signal preparation except conversion to temperatures is used for the signals presented in the following.

MTCP probe signals are conditioned as follows. Typical discrete frequencies like line noise etc. are not present in the signal because of careful shielding and design of the electronics used. Even though the entire signal chain has been optimized to achieve an optimum signal to noise ratio, some noise can be found in the signal. The observed level of noise is partly the result of the signal bandwidth which is exceptionally large for temperature measurements. The thermal noise voltage U_{noise}, for example, can be calculated by $U_{\text{noise}} = \sqrt{4kTR\Delta f}$ with the Boltzmann constant k, the temperature T, the electric resistance R and the bandwidth Δf [23]. Common techniques like averaging or application of low-pass filters cannot be used here as the important signal dynamics will be altered (an example is given in [8]).

These drawbacks can be overcome with the application of wavelets for signal denoising. This method enables reduction of noise while preserving the characteristic signal features. The observed noise floor of the raw signal (measured in Kelvin peak-to-peak) after conversion to temperature is typically between about ± 0.04 to ± 0.1 K. Application of wavelet denoising results in a reduced noise level of about ± 0.01 K or less. The next step is the removal of outliers. These are very rare (most files do not have a single outlier) but would result in errors during the statistical analysis which will be presented in the future. Outliers are defined here as temperature peaks with values well beyond the range of temperatures possible from theory (i.e. well below T_{sat} or above T_{heater}). After the mentioned signal conditioning, the signals are converted to temperatures as outlined in Section 2.5.

For the mapping of the measured probe-temperatures to either the liquid or the vapor phase, the MOP provides valuable information on the state of phase at the probe tip. Due to the radial distance between the probes (see Fig. 2)—which is necessary to avoid a liquid film between both probes (see Section 2.5)—a phase change does not occur at the same moment at the MOP and the MTCP in general. The time deviation is a function of the bubble diameter, the flow properties (turbulence etc.) and the radial probe distance. It is expected to be minimal for large bubbles and low turbulence. Anyhow, the temperature traces presented in Section 4.4 enable a clear determination of the instances of phase change at the probe tip. Corresponding MOP and MTCP signals are not presented because the direct interpretation could be misleading for short signal periods as shown in the following.

4. Results

4.1. Boiling curves

The steady-state boiling curves of isopropanol and FC-3284 are depicted in Figs. 3 and 4, respectively. The duration of the measurements for a point of the boiling curve is mostly 60 s, which also includes the time for the microsensor measurements. All measurement durations are well above the time needed for good reproducibility. Both curves are measured at $p = 0.106$ MPa.

As can be expected from theory, the boiling curve of isopropanol exhibits higher heat flux values than the FC-3284 boiling curve. Higher superheats for comparable setpoints on the boiling curve are found for isopropanol when compared to FC-3284. Differences in the overall shape of the boiling curves are obvious. A difference is also present in the transition boiling region. While the curve for FC-3284 is smooth in this region, a discontinuous jump at about $\Delta T = 43$ K is present for the isopropanol boiling curve. This difference is not important for the purpose of this paper; for a discussion of the effect we refer to [6].

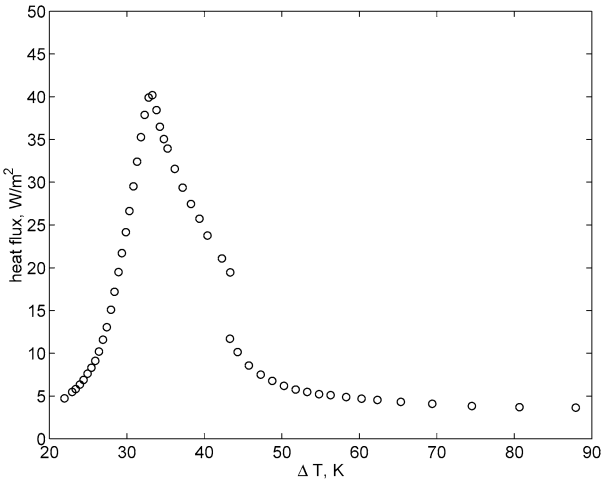

Fig. 3. Boiling curve of isopropanol.

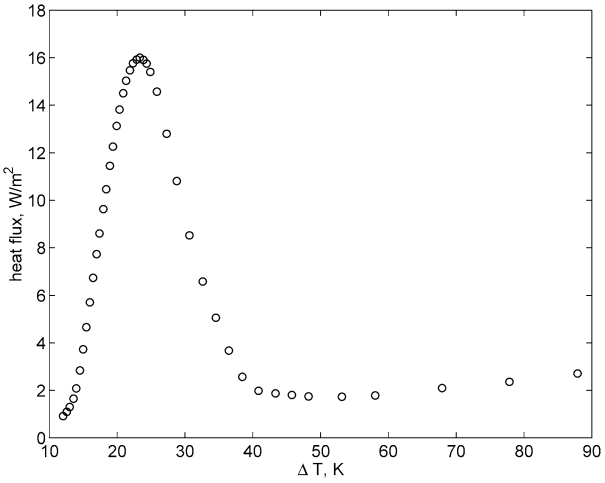

Fig. 4. Boiling curve of FC-3284.

4.2. Temperature fluctuations at the heater surface

Typical traces of the measured temperature at two neighboring microthermocouples (MTCs) are depicted in Figs. 5–8 for nucleate boiling, CHF, transition- and film boiling. Each figure depicts traces for isopropanol (top plot) and for FC-3284 (bottom plot). The plotted signals represent the temperature inside the heater at a position 3.6 μm below the heater surface. The measured temperature at the MTC location is very close to the real surface temperature with respect to value and dynamics which has been shown by a solution of the inverse heat conduction problem [24]. The horizontal distance between the thermocouple junctions of the neighboring MTCs Nos. 7 and 8 of the MTC array is 211.6 μm (for more details see [8]).

The temperature traces in Figs. 5–8 are typical examples of the temperature dynamics, although a complete representation of the signal characteristics as well as its statistics for the vastly different time scales involved would require far more plots than possible here.

As can be expected, the amplitude of the temperature fluctuations measured with isopropanol increases with increasing wall superheat. This also holds for FC-3284, but at a generally

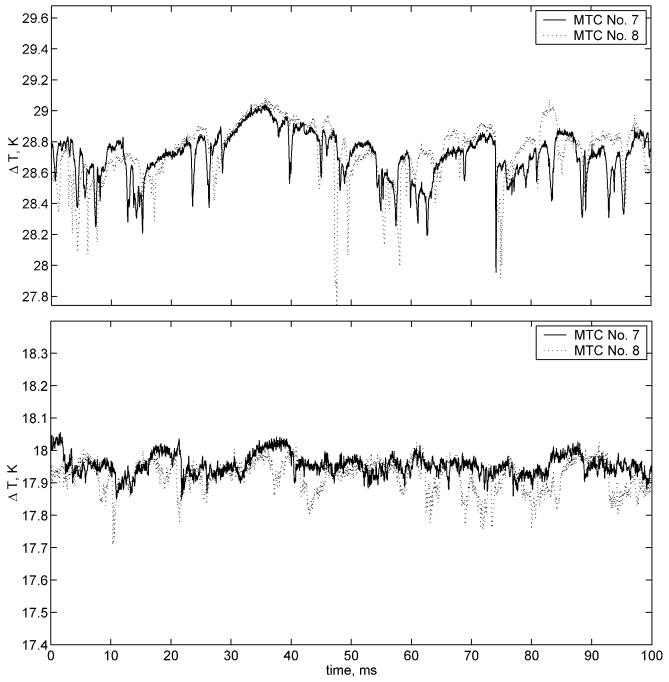

Fig. 5. Temperatures at MTCs Nos. 7 and 8 in nucleate boiling; top: isopropanol, bottom: FC-3284. Horizontal distance 7 → 8: 211.6 μm.

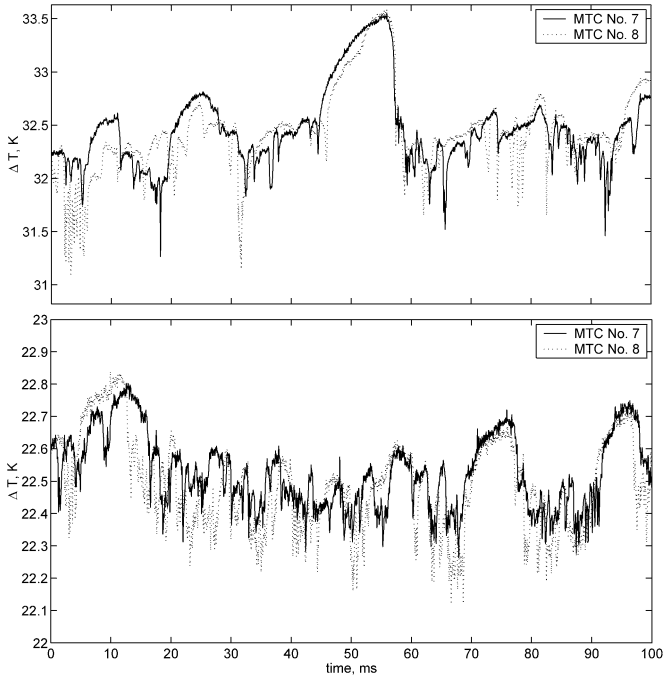

Fig. 6. Temperatures at MTCs Nos. 7 and 8 at CHF; top: isopropanol, bottom: FC-3284. Horizontal distance 7 → 8: 211.6 μm.

smaller fluctuation amplitude. The latter is not very surprising since the measured mean heat flux is also smaller. The observed dependency of the fluctuation amplitude on the heater superheat can be expected because the theoretical limit for a temperature drop is $\Delta T_{\text{fluct,max}} = T_{\text{surface,max}} - T_{\text{sat}}$ for saturated boiling conditions. Thus, the theoretical limit for a fluctuation amplitude increases with increasing superheat, except for film boiling where no wetting of the surface occurs.

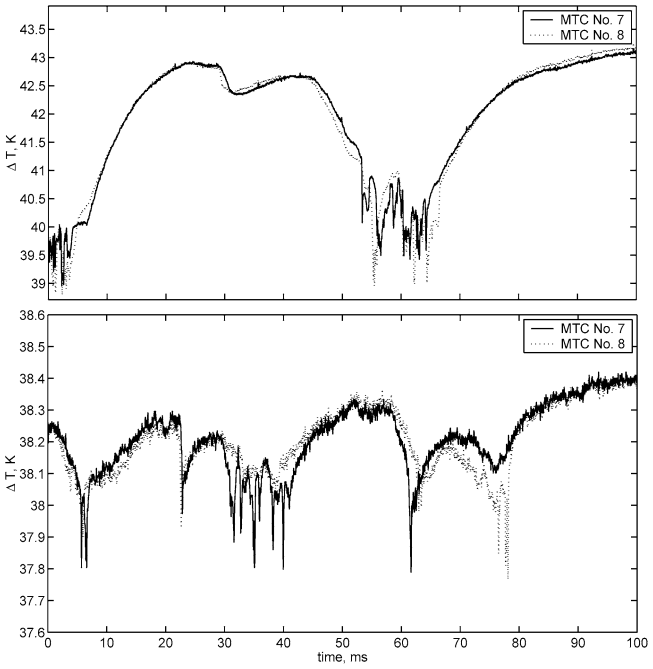

Fig. 7. Temperatures at MTCs Nos. 7 and 8 in transition boiling; top: isopropanol, bottom: FC-3284. Horizontal distance 7 → 8: 211.6 μm.

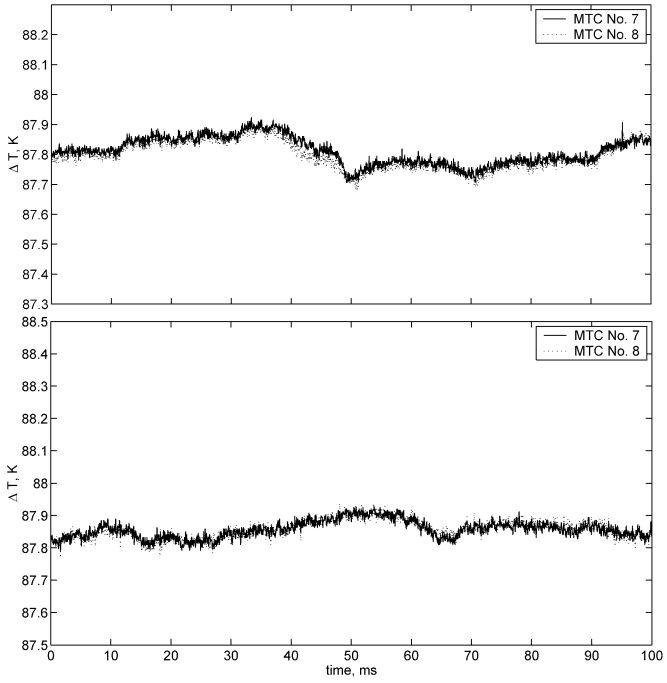

Fig. 8. Temperatures at MTCs Nos. 7 and 8 in film boiling; top: isopropanol, bottom: FC-3284. Horizontal distance 7 → 8: 211.6 μm.

The number of temperature fluctuations per time due to nucleation or a rewetting event changes also along the boiling curve. It increases between low heat flux nucleate boiling and around CHF. Increasing the wall superheat further leads to a decrease of the number of fluctuations until they vanish at the Leidenfrost point. Beyond the Leidenfrost point in the film boiling region, no comparably pronounced temperature drops can be found in the signal. Obviously, surface wetting does not take place beyond the Leidenfrost point. Assuming the ergodic hypothesis to be valid for our boiling system in this regime, no direct liquid contacts should occur on the entire heater surface.

Sharp temperature drops are detected in the region between low heat flux nucleate boiling and transition boiling close to the Leidenfrost point. A rapid temperature decrease points most likely to ongoing nucleation and subsequent growth of a bubble directly above or close to the MTC junction in nucleate boiling. In transition boiling, a temperature drop can be interpreted as local rewetting of the surface and subsequent nucleation and growth of small bubbles followed by a creation of larger vapor patches. The probability of a vapor patch to be present at the surface is commonly accepted to increase with increasing superheat from high to low heat flux transition boiling. The decreasing number of temperature fluctuations with increasing heater temperature in transition boiling fits with this understanding of transition boiling. Furthermore, also the results of optical probe measurements support this reasoning (see Section 4.3).

The local temperature transient at the MTC position during a rewetting period (transition boiling) can exceed $-30\,000\ \mathrm{K{\cdot}s^{-1}}$ for isopropanol. We compared the resulting temperature amplitudes (see Fig. 7) with those which would be obtained if only unsteady heat conduction within the boiling liquid acted as a heat transfer mechanism during a rewetting event. If a vapor covered surface is wetted with saturated liquid, a contact temperature of -0.67 K for isopropanol and -0.36 K for FC-3284 below the surface temperature would be obtained during the contact if heat conduction between two semi-infinite bodies is assumed (assumptions: 1-D, saturated fluid, massive copper heater). Since observed temperature drops (see e.g. Fig. 7) are higher than these calculated values, unsteady conduction between liquid and heater cannot explain the measured temperature drops.

Furthermore, it is very unlikely that the temperature drops observed in transition boiling even near the Leidenfrost point are caused by local conduction through an extremely thin vapor film, i.e. without wetting of the surface which is sometimes postulated in the literature. This becomes obvious by a simple conservative estimate. We calculate the average local heat flux required to generate the temperature drops observed first. Then, we calculate the vapor film thickness needed to cause such heat flux by conduction only. The film would have a thickness of about 0.2 μm to facilitate such a pronounced temperature drop. This thickness is less than the surface roughness of the heater ($P_t = 0.88$ μm) and we do not believe that the film would not be pierced by the peaks on the surface.

Highly turbulent convection of liquid as explanation for the temperature drops along the boiling curve up to the Leidenfrost point can be excluded as this effect can certainly not cause such steep *and* localized temperature fluctuations. Thus, evaporation, i.e. the direct generation of vapor at the surface in the nearfield of the MTC, is likely to be the only realistic explanation.

This finding fits also with results gained from a theoretical analysis in [25] where the processes are investigated which take place if bubbles grow at a heated wall at nucleate boiling. [25] found a localized zone at the bubble foot—the so-called

micro region—with extremely high heat fluxes. More recently, this finding was confirmed also experimentally using a steady evaporating meniscus, see [2]. It is likely, that evaporation in the micro region cause the pronounced temperature drops observed, the more as they are very local events. Even at the neighboring MTCs (distance 211.6 μm) some fluctuations occur independently at both MTC junctions. These sharp temperature drops are mostly not well correlated. On the other hand, slower temperature changes—slow compared to the very rapid changes during nucleation or rewetting—are much better correlated at neighboring MTCs, see Fig. 6 and also Fig. 7. This finding points most likely to the existence of larger structures on the surface like dry patches in transition boiling.

Although the theory of micro region evaporation was developed for single bubbles, the principal findings are expected to describe also the fundamental processes at the three-phase contact line between the heated wall, liquid and vapor in all boiling regimes with surface wetting in general. This approach has been employed to model pool boiling along the entire boiling curve successfully in [24].

Periods with high temperature in transition boiling are often simultaneously observed by far more than just two neighboring MTCs. A visualization of such an event (in this case close to CHF in nucleate boiling) can be found in Fig. 14 of [8] (it is recommended to use the online version on http://www.sciencedirect.com to view the figure in color). Therefore, the area covered by such unstable vapor patches can be expected to be partly in excess of 1 mm^2 at CHF, and even larger at higher wall superheats. If the patch is larger than 1 mm^2 a real identification of the size is difficult, because they exceed the size of the MTC array. Within these dry patches the measured temperatures at neighboring MTCs can be expected to be similar because the thermal conduction within the heater is strong relative to the local surface heat flux. The same holds for areas without bubble nucleation in low heat flux nucleate boiling because natural convection certainly cannot cause localized pronounced temperature drops on a heater with high thermal conductivity and thermal capacity.

4.3. Experiments with micro optical probes

The mean void fraction α_v at a probe distance z is given as the average value of the two-valued phase indicator function (PIF). All void fractions presented in this paper are calculated using the entire length of the signal, which is typically 60 s or 1.2×10^7 signal samples. In the following, the void fraction measured by the lowest probe of the 4-tip MOP is presented. The mean void fraction is plotted for probe positions from 5 μm (for FC-3284) or 8 μm (for isopropanol) to 2 mm above the heater surface for nucleate boiling, CHF, transition- and film boiling in Figs. 9–12, respectively. In each diagram, results for both test fluids—isopropanol and FC-3284—are plotted together for the same boiling regime and comparable dimensionless heat fluxes $q^* = \dot{q}/\dot{q}_{\mathrm{CHF}}$. Because of the limited space available, we focus in this chapter on the two phase zone close to the heater where the most important mechanisms take place.

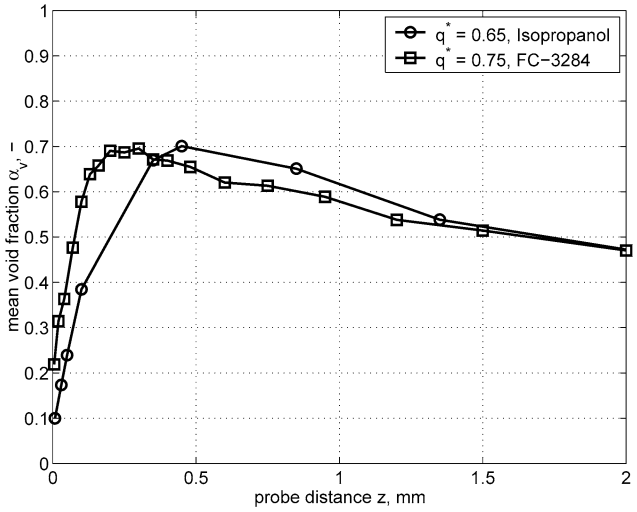

Fig. 9. Mean void fraction for nucleate boiling measured with isopropanol and FC-3284.

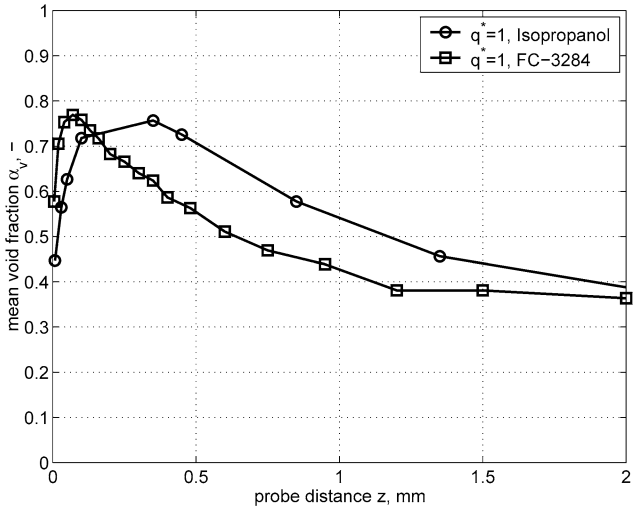

Fig. 10. Mean void fraction at CHF measured with isopropanol and FC-3284.

The void fraction at the closest measured distance to the heater increases from low surface superheat towards CHF. For all the measured boiling points along the boiling curve between nucleate boiling and CHF (Figs. 9 and 10), a liquid rich layer has been found near the heater surface. A distinctive local maximum of the void fraction can be seen for all points between nucleate boiling at moderate heat flux and CHF. The location of this maximum moves towards smaller heater distances for increasing surface superheat and heat flux. If we define the position of this void fraction peak as the upper end of the liquid-rich zone, its thickness decreases monotonically with increasing superheat taking into account our entire data set. A decrease of α_v close to the heater is also found in high heat flux transition boiling (not shown here, see [8]). We believe that the vapor-rich zone around the void fraction maximum is on the one hand linked to some kind of bubble departure diameter [6] if even the term “bubble departure diameter” is applicable to high heat flux boiling with all kinds of coalescence etc. On the other hand, this vapor-rich zone could also play a significant role for a changing

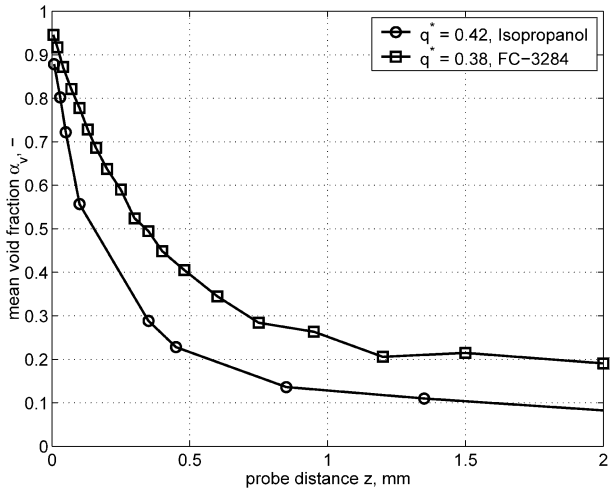

Fig. 11. Mean void fraction for transition boiling measured with isopropanol and FC-3284.

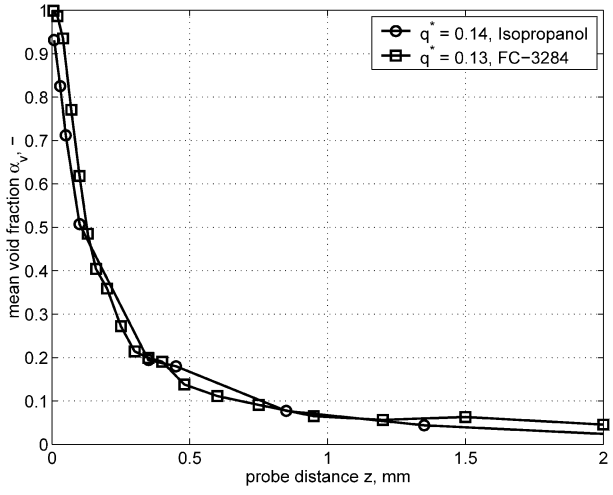

Fig. 12. Mean void fraction for film boiling measured with isopropanol and FC-3284.

fraction of convective heat transfer in the liquid to the overall heat transfer. This will be discussed in the next section.

The situation is different in low heat flux/high superheat transition boiling and also in film boiling, respectively (Figs. 11 and 12). In these regions, no drop of the local void fraction close to the heater surface can be found. Here, the measured maximum of the void fraction is located at the smallest measured distance pointing to the existence of large fluctuating vapor patches in transition boiling and a stable vapor film in film boiling at the surface. In transition boiling α_v is < 1, since liquid with sufficiently large kinetic energy may reach the heater surface and may rewet the surface which is observed by the MTCs (see Section 4.2). In film boiling, surface rewetting has not been observed by the MTCs. An extrapolation of the MOP signals to $z = 0$ in Fig. 12 tends to $\alpha_v = 0$.

4.4. Microthermocouple probe experiments

Temperature traces measured with isopropanol are depicted in Fig. 13 for low heat flux nucleate boiling, in Fig. 14 for film boiling, in Fig. 15 for CHF and in Fig. 16 for transition boiling. Each figure depicts signals at a distance of 9 mm (top) and 0.1 mm (bottom) of the probe. Note that Figs. 13 and 14 depict time intervals of 400 ms and Figs. 15 and 16 of only 100 ms. We selected these different durations for the sake of best representation of the short-term dynamics in these regions. The observed events occur on a relatively wide range of time and temperature scales and consequently the plots should not be considered to completely represent the entire boiling process. Microthermocouple (MTCP) experiments with FC-3284 have also been carried out but are not presented here for space reasons.

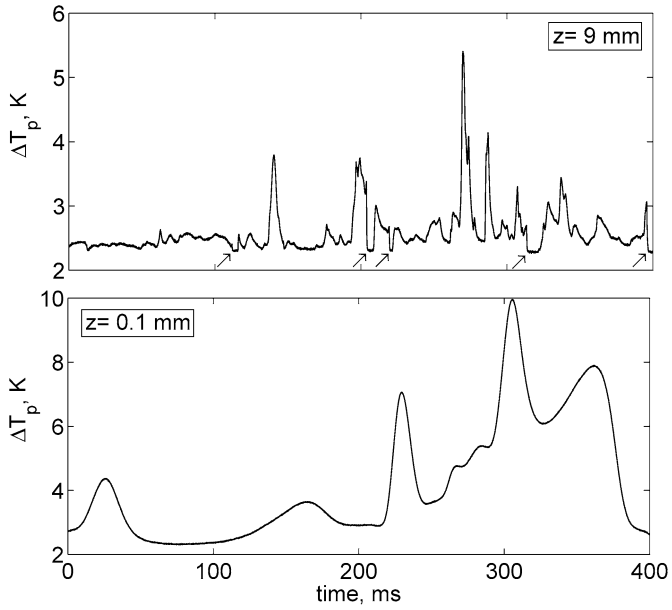

Fig. 13. Measured local fluid temperature in nucleate boiling (3.5 W·cm^{-2}, see Fig. 3) at 9 mm (top) and 0.1 mm (bottom) distance to heater surface (isopropanol); arrows indicate vapor contacts; $\Delta T_p = T_{\text{probe}} - T_{\text{sat}}$.

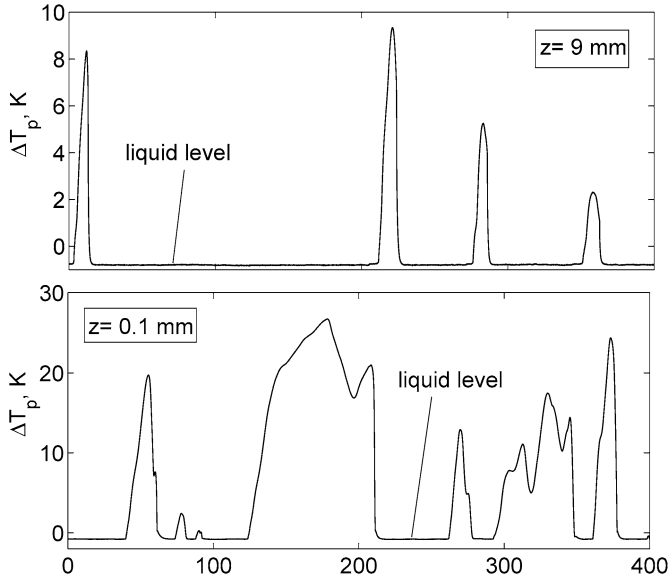

Fig. 14. Measured local fluid temperature in film boiling ($\Delta T = 71$ K, see Fig. 3) at 9 mm (top) and 0.1 mm (bottom) distance to heater surface (isopropanol); $\Delta T_p = T_{\text{probe}} - T_{\text{sat}}$.

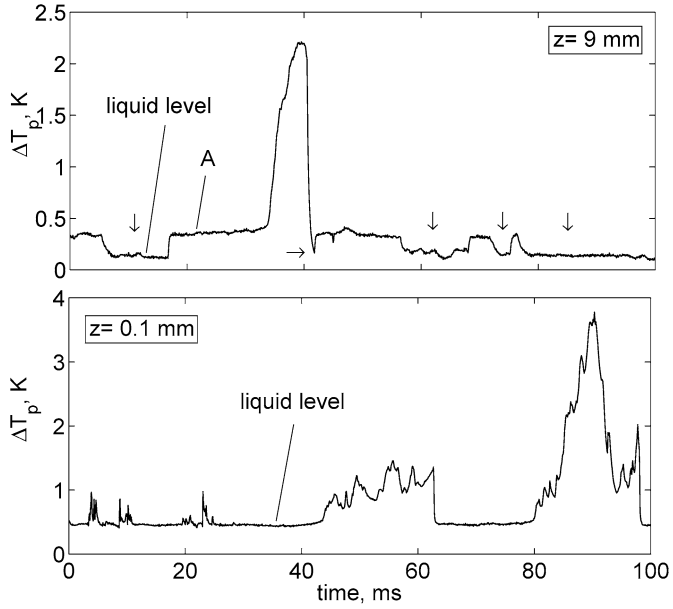

Fig. 15. Measured local fluid temperature at CHF at 9 mm (top) and 0.1 mm (bottom) distance to heater surface (isopropanol); arrows indicate liquid contacts; **A**: see Section 4.4.5; $\Delta T_p = T_{\text{probe}} - T_{\text{sat}}$.

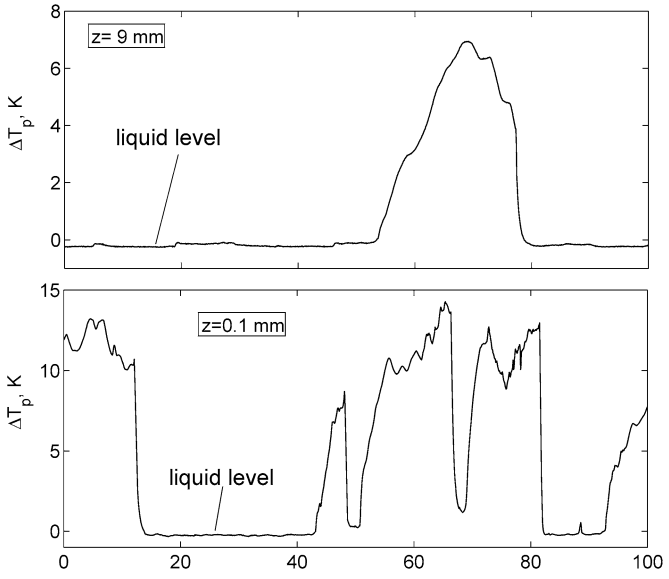

Fig. 16. Measured local fluid temperature in transition boiling ($\Delta T = 42$ K) at 9 mm (top) and 0.1 mm (bottom) distance to heater surface (isopropanol); $\Delta T_p = T_{\text{probe}} - T_{\text{sat}}$.

4.4.1. Nucleate boiling

In nucleate boiling at low heat flux (3.5 W·cm^{-2}, see Fig. 3), strong temperature fluctuations are found in the liquid, Fig. 13. The liquid is always superheated, with maximum dimensionless superheats $T_p^* = (T_{\text{probe,max}} - T_{\text{sat}})/(T_{\text{heater}} - T_{\text{sat}})$ up to 0.8. Vapor contacts were not observed at $z = 0.1$ mm but are found at $z = 9$ mm distance. During a vapor contact, which is indicated by the attached MOP the temperature drops down quite fast. However, the lowest temperature measured inside the vapor ($\Delta T_p \approx 2$ K) is always above saturation temperature. It is also certainly above the minimum value needed for a bubble of the estimated diameter to exist according to theory. The temperature during a vapor contact remains approximately constant in nucleate boiling. This is different in other boiling regimes, as will be shown later. After a vapor contact, the probe heats up again quite rapidly.

The temperature changes within the liquid at low heat flux and close to the heater surface ($z = 0.1$ mm) are relatively slow. This is reasonable as the fluctuations are expected to be caused by natural convection and also by improved convection due to bubble nucleation, growth and rise. However, at the small distance, the temperature field seems to be not much affected by turbulence due to bubble dynamics in the present case. At 9 mm probe distance, the fluctuations are much more rapid. The measured liquid superheat near to the interface can be up to 5.5 K (close to 4 K superheat near an interface can be found in Fig. 13, top; see 2nd arrow from left). This holds even if we take into account that the measured temperature inside the bubble can potentially be affected by errors because of a liquid film which may be present on the MTCP probe surface after penetrating the interface. It is currently not fully understood whether this effect is important—and if this is the case, to which extent—or not (for a detailed discussion of the measurement accuracy see Section 4.4.5).

Temperature fluctuations at 9 mm probe distance within the liquid are much faster than close to the heater which can be explained as follows. The level of turbulence in low heat flux nucleate boiling (isolated bubbles) is expected to increase with increasing distance to the heater because the bubbles are accelerating. The bubbles should therefore mix the liquid which leads—as observed—to a better temperature equalization within the fluid. The total temperature fluctuation amplitude should therefore decrease with increasing distance. It is furthermore likely that further away from the superheated boundary layer above the surface the temperature amplitudes are anyway smaller than very near to the surface.

4.4.2. Film boiling

In film boiling, see Fig. 14, the characteristics are opposed to the behavior in nucleate boiling at moderate heat flux. Unlike nucleate boiling, the liquid temperature remains constant. It is about the pool temperature and approximately independent of the probe position. The liquid temperature is slightly subcooled by about 0.5 K which represents the main pool conditions. A slight increase towards saturation temperature is detected for decreasing distance of the probe. The measured vapor temperature exhibits very large fluctuations. Vapor superheats of more than 40 K have been found at a heater superheat less than 80 K. As to be expected the measured maximum superheat inside the vapor decreases with increasing probe distance.

In film boiling no liquid contact occurs at the heater surface, which is proved by the MTC-signals. The absence of liquid contacts at the heater surface thus prohibits the liquid to be heated above saturation temperature as observed by the MTCP. The maximum possible liquid temperature can be expected to be saturation temperature at vapor–liquid interfaces. This is confirmed by the measurements which show the small subcooling in our pool (0.5 K). For the vapor, we get quite dif-

ferent conditions. The vapor film at the heater surface has direct contact to the hot surface, consequently its temperature is well above saturated conditions. If a bubble leaves the film it obviously contains this superheated vapor. It is reasonable—and confirmed by the experiments—that with increasing probe distance the vapor cooles down due to convection and conduction inside the bubbles since the interface temperature of the bubbles can be assumed to be at about saturated conditions. Because of the small heat capacity of the vapor inside the bubble the total heat removed from the vapor and transferred to the interface until saturation is reached is small.

In Fig. 14 different durations of vapor contacts for 9 mm and 0.1 mm probe distance are observed. At 9 mm distance, the probe certainly detects large rising bubbles. At 0.1 mm distance, both short and long vapor contacts are found. Here, the probe is possibly located near to the interface of the wavy vapor film at the heater surface. Contacts with the relatively slow-moving interface—especially for the case of a bubble growing and departing from the film with low initial velocity—are expected to last longer than for a rising bubble.

4.4.3. Critical heat flux

At CHF, as can be expected from the MOP experiments, an increased number of vapor contacts can be found. This is confirmed by the plots in Fig. 15. Note, that the plotted interval in Figs. 15 and 16 is now 100 ms. As opposed to the characteristics in nucleate boiling, the detected vapor temperature exhibits some temperature fluctuations with much higher amplitudes than observed in nucleate boiling. Furthermore, vapor temperature at CHF appears to be always higher than the liquid temperature. The relatively weak increase of surface superheat between nucleate boiling and CHF ($\approx$10 K, see Fig. 3) can certainly not explain this characteristic change. As described in the previous chapter, very high vapor superheats are observed in the film boiling regime where vapor covers the entire surface. If we assume unstable vapor patches around CHF to exist for short periods on a given surface area, the vapor above this patch would gain a higher temperature. After lift off, this elevated vapor temperature can be expected inside the bubble for a short period until heat transfer to the interface causes the temperature to decrease. The existence of unstable vapor patches even below CHF has been proven with the MTC-array (see Fig. 14 in [8]). Therefore, the measured vapor temperature excursions can be assumed to be the result of the dry areas on the heater surface. The transition from "hot liquid" and "cold bubbles", as observed in low heat flux nucleate boiling (Fig. 13) to the opposite case at CHF and towards film boiling occurs most likely gradually.

The liquid temperature at CHF fluctuates much less than in nucleate boiling. We assume that this is due to the strong increase of nucleation site density and thus increased turbulence and interfacial area density. Hence, increased mixing as well as locally available interfaces which act as "heat sinks" lead to the observed liquid temperature characteristics.

A discussion of the intermediate level (A) in Fig. 15, top, is given in Section 4.4.5.

4.4.4. Transition boiling

Temperature traces measured in steady-state transition boiling are depicted in Fig. 16. The sequences plotted represent low heat flux/high superheat transition boiling ($\Delta T = 42$ K, Fig. 3). Thus it is not surprising that the signal has similarities with those observed in film boiling. But there are also important differences. First, the maximum detected vapor superheat in transition boiling is less than in film boiling if we compare the signals at both distances. This finding is reasonable as the driving ΔT is lower. Second and more important, the signal dynamics are different. This is more obvious at a probe distance of 0.1 mm. The temperature traces exhibit many rapid fluctuations within the vapor—and also more vapor contacts—and the "smoothness" of the signal is lower than observed in film boiling. Furthermore, the signals appear more irregular than in film boiling. Both findings indicate that some mechanism involved generates more "turbulence" or, in other words, a locally less-steady heat transfer mechanism. Analysis of MTC experiments in transition boiling (see Section 4.2) prove that rewetting and dryout processes are very rapid in this region. Because the driving ΔT is very large compared to nucleate boiling, the local evaporation process is very fast. Thus, the local vapor generation during the short and intermittent surface wetting events is expected to be associated with local high vapor velocity. This leads to a high level of turbulence and thus rapid temperature fluctuations within the vapor as detected by the MTCP probe. It is furthermore not impossible that very small droplets created by the explosive evaporation process touch the probe during its contact with the vapor phase. This mechanism may also affect the vapor temperature behavior during a local dryout of the heater surface at about CHF (see Fig. 15).

4.4.5. Discussion of microthermocouple probe measurement accuracy

For the complex temperature measurement being carried out here the real measurement accuracy is not easy to determine. The accuracy is affected—additionally to the usual error components like systematic and statistic errors—also by the thermal inertia of the sensor and a liquid film on the MTCP which could be present after a liquid $\rightarrow$ vapor phase change. Our analysis of the signals reveal that amplitude errors due to insufficient response time of the sensor are not very important. This holds for measurements within the liquid and for a vapor $\rightarrow$ liquid phase change. It holds also for measurements within vapor—which is expected to be the most critical measurement situation with regard to response time—or for a liquid $\rightarrow$ vapor phase change. For any of the possible cases, signal periods are found during which the temperature settles and/or exhibits faster fluctuations superimposed to the general trend. These superimposed fluctuations would be impossible to detect for a response-time governed temperature signal (a good example is given in Fig. 16; note that the amplitude at 9 mm is comparable to film boiling but plotted for a shorter duration here). Any error due to MTCP response time would lead to an underestimation of the temperature amplitude. However, the rate of temperature change, especially during a phase change, could be even faster in reality than the measured ones. Calculation of the power spectral

density reveals that high frequency signal components above 10 kHz due to boiling are present in the temperature signal. Thus, filter cutoff frequency (12.5 kHz) could be too low to let pass the highest frequency components of real temperature changes detected by the probe.

Measurement errors due to a liquid film atop the MTCP surface are difficult to quantify. This holds even more as we found sequences which point to the presence of a vapor film and also sequences which contradict this assumption. Careful experiments and detailed dynamic simulations of the MTCP are necessary to obtain the definite dynamical effects if a liquid film is present atop the MTCP surface. These tasks are beyond the scope of our present investigation but the effects will be analyzed in more detail in the future.

Here we discuss briefly some possible cases in order to get a rough estimate of the error bounds. For a dry probe, the measured temperature should not be affected except due to the dynamical properties of the sensor and the electronics used. For a wetted probe, we consider two different cases which are representative for the nucleate and film boiling regimes. Here, we assume the vapor pressure inside the bubble to be at pool pressure $p = p_\infty = p_{\text{bubble}}$ regardless of the pressure difference and superheat necessary to sustain a bubble due to the interfacial tension at the bubble's surface since the difference is very small for our conditions.

(1) A phase change superheated liquid → saturated vapor takes place at the probe tip. Unlike interfacial tension at the interface of the bubble itself, interfacial tension may play an important role at the surface of the film atop the probe as the diameter of the probe is very small (≈16 μm). If we assume the shape at the probe tip to be semi-hemispherical, we can calculate the pressure difference across the interface using the Young–Laplace equation [26]. The pressure difference under these conditions is about 46 mbar (for isopropanol) which corresponds to a shift of the film's saturation temperature of about +1 K. Most of the pressure difference acts on the liquid side but the pressure of the vapor above the interface with convex curvature is also affected—its pressure is slightly increased with respect to p_{bubble}. This leads to a complex coupled problem including evaporation at the interface, heat transfer from the interface to the bubble due to conduction and convection as well as mass transfer due to vapor flow perpendicular to the interface. The process is even more complicated as the interface's curvature and thus film pressure changes with a change of film thickness and probably mass transfer resistance at the interface plays also a role.
(2) A phase change saturated liquid → superheated vapor takes place at the probe tip. We assume the same conditions regarding the pressure conditions. Unlike for the case (1), the direction of the heat flow both within the sensor and more important also inside the vapor are in the inverse direction here. Still, we have the coupled mechanisms of heat and mass transfer at the interface. Being opposed to the case (1), we have a significant temperature gradient between bubble and film which definitely forces the liquid film to evaporate and consequently delays the establishing of the real vapor temperature.

In low heat flux nucleate boiling (case (1)) we measure always a higher temperature than $T_{\text{sat}} + 1$ K thus is seems likely that the vapor temperature is not saturated but superheated. At present, we cannot estimate its true superheat in nucleate boiling with a liquid film present at the probe tip. In boiling regimes where superheated vapor and about saturated liquid can be present (case (2) which is applicable to CHF, transition boiling, film boiling and possibly high heat flux nucleate boiling), the real vapor temperature is expected to be measured after some delay caused by the time necessary to evaporate the film. This means for the conditions assumed that a liquid film could lead at the worst only to an underestimation of the real temperature. The evaporation of a liquid film atop the probe is expected to cause the intermediate temperature level for the vapor (denoted by "A" in Fig. 15, top). The temperature here is about constant for about 15 ms until the temperature rises quite fast. This behavior can be explained with the dryout of a liquid film atop the MTCP.

5. Conclusions

Several microsensors for measurements of local characteristics in boiling have been developed and applied in the heater as well as in the two-phase flow region very close to the heater surface. Microthermocouples (MTCs) below the heater surface (3.6 μm) as well as a micro optical probe (MOP) and a microthermocouple probe (MTCP) above the heater surface provide measurement information with very good spatial and temporal resolution. Information of this kind is a necessary prerequisite for the development of mechanistic models for all boiling regimes along the lines presented in [24]. Measurements were carried out with saturated isopropanol and FC-3284 at 0.106 MPa. After analyzing the data, some conclusions on qualitative boiling mechanisms can be drawn:

(1) *Nucleate boiling*. Very rapid temperature drops and a slower recovery period occur locally at the surface and below. The number of those drops as well as their amplitude increases with mean surface superheat. They are linked with bubble nucleation and growth above a MTC. Fluctuations at neighboring MTCs at a distance of 211.6 μm appear to be often independent. Measurements with the MOP within the fluid above the heater reveal that a liquid rich layer is present at the surface. Its thickness decreases with increasing wall superheat. The liquid above the heater is significantly superheated with pronounced but slow temperature fluctuations at low heat flux (MTCP). Thus, at low heat fluxes with a small number of active nucleation sites a significant portion of the total heat flux is transferred by convection. For higher heat fluxes, faster liquid temperature fluctuations with smaller amplitudes at a lower liquid temperature level have been found. For the vapor, the opposite trend is observed: its temperature is less than the liquid temperature in low ΔT nucleate boiling but increases with

increasing wall superheat. Close to CHF, rare temperature excursions are detected locally at the heater surface measured by MTCs and also inside the vapor phase above the heater (MTCP). Both findings (for vapor and heater temperature) point to the existence of dry patches in this region.

(2) *Critical heat flux*. At CHF, temperature fluctuations at the surface occur more frequently and with a higher amplitude than in nucleate boiling (MTC). MOP measurements reveal that a liquid rich zone is still present above the heater. Its thickness is less than observed in nucleate boiling and is smaller for FC-3284 than for isopropanol. The measured local liquid temperature (MTCP) is very close to saturation temperature. The vapor temperature inside the bubbles is always above saturation. Superheatings of up to 10 K (MTCP) are observed. Dry patches occur at the surface.

(3) *Transition boiling*. In transition boiling, the number and duration of periods without rapid temperature fluctuations but high temperature level (MTCs) increases with increasing superheat. Very rapid temperature drops with drop rates in excess of $-30\,000$ K·s^{-1} are also found (MTCs, isopropanol). These temperature drops can be explained with local rewetting and subsequent growth of vapor at the surface. Measurements above the surface (MOP) still document the presence of a thin liquid rich layer close to CHF, but not for higher wall superheats. Superheated vapor inside the bubbles is measured above the surface with longer duration and increased maximum temperature compared to CHF (MTCP). The liquid temperature above the surface is at pool temperature already at a distance of 0.1 mm to the surface.

(4) *Film boiling*. Here, surface temperature fluctuations are very weak (MTCs), thus no surface wetting takes place. The liquid temperature above the heater is always at about pool conditions, even very close to the surface (MTCP). At a distance of 0.1 mm to the surface vapor superheats in excess of 40 K at wall superheats <80 K have been found. The superheat in the bubbles decreases with increasing distance to the surface due to heat transfer to the interface.

(5) For all measurements we have analyzed so far, the signals appear to change their characteristics smoothly from one boiling regime to the next along the entire boiling curve. As a general trend, the vapor temperature inside the bubbles increases with increasing heater superheat between low heat flux nucleate boiling (vapor temperature slightly above saturation but significantly smaller than liquid temperature) and film boiling (vapor temperature much higher than liquid temperature which is very near to saturation).

This report summarizes only the first examination of a huge amount or raw data. For example, the data base for Section 4.4 amounts to about 70 GB even in binary format. It is expected that further examination and additional experiments yield quantitative results such as spacial and temporal characteristics of dry patches, spacial and temporal characteristics of surface heat fluxes by solving the inverse heat conduction problem (see [24]), bubble dynamics at different distances to the surface and other important quantities required to develop mechanistic models.

Acknowledgements

The authors highly appreciate financial support by the Deutsche Forschungsgemeinschaft (DFG) in the frame of a joint research project on fundamentals of boiling heat transfer. The project was supported with bidirectional optical fiber units Bidi® by Infineon AG, Germany. The test fluid PF-5052/FC-3284 was provided by 3M Company. The authors express their gratitude towards the students J. Judex and J. Pöthke who helped to carry out measurements and data analyses.

References

[1] D.B.R. Kenning, Y. Yan, Pool boiling heat transfer on a thin plate: features revealed by liquid crystal thermography, Int. J. Heat Mass Transfer 39 (1996) 3117–3137.
[2] C. Höhmann, P. Stephan, Microscale temperature measurement at an evaporating liquid meniscus, J. Exp. Therm. Fluid Sci. 26 (2002) 157–162.
[3] I. Golobic, E. Pavlovic, J. von Hardenberg, M. Berry, R.A. Nelson, D.B.R. Kenning, L.A. Smith, Comparison of a mechanistic model for nucleate boiling with experimental spatio-temporal data, Chemical Engrg. Research and Design, Part A: Trans. Inst. Chem. Engineers 82 (2004) 435–444.
[4] U. Kleen, Untersuchungen zum Übergangssieden von strömendem Wasser an elektrisch erwärmten Heizflächen mit temperaturgeregelter Wärmezufuhr, PhD thesis, Technische Universität Berlin, Germany, 1984.
[5] A. Bar-Cohen, A. Watwe, M. Arik, Pool boiling critical heat flux in dielectric liquids, in: Proc. 5th Int. Boiling Heat Transfer Conf., Montego Bay, Jamaica, 4–8 May 2003.
[6] H. Auracher, W. Marquardt, Heat transfer characteristics and mechanisms along entire boiling curves under steady-state and transient conditions, Int. J. Heat Fluid Flow 25 (2004) 223–242.
[7] M. Buchholz, H. Auracher, Microsensors to study temperature fluctuations near the heater surface and two-phase flow characteristics, in: Proc. 8th UK Nat. Heat Transfer Conf. 2003.
[8] M. Buchholz, T. Lüttich, H. Auracher, W. Marquardt, Experimental investigation of local processes in pool boiling along the entire boiling curve, Int. J. Heat Fluid Flow 25 (2004) 243–261.
[9] J. Blum, W. Marquardt, H. Auracher, Stability of boiling systems, Int. J. Heat Mass Transfer 39 (1996) 3021–3033.
[10] A. Luke, Thermo- and fluiddynamics in boiling, connection between surface roughness, bubble formation and heat transfer, in: Proc. 5th Int. Boiling Heat Transfer Conf., Montego Bay, Jamaica, 4–8 May 2003.
[11] M. Jakob, W. Fritz, Versuche über den Verdampfungsvorgang, Forschung, Mitteilung aus der Physikalisch-Technischen Reichsanstalt 2 (12) (1931) 435–447.
[12] B.D. Marcus, D. Dropkin, Measured temperature profiles within the horizontal surface in saturated nucleate pool boiling of water, J. Heat Transfer 37 (1965) 333–341.
[13] J.R. Wiebe, R.L. Judd, Superheat layer thickness measurements in saturated and subcooled nucleate boiling, J. Heat Transfer 94 (1971) 455–461.
[14] S.J.D. van Stralen, W.M. Sluyter, Local temperature fluctuations in saturated pool boiling of pure liquids and binary mixtures, Int. J. Heat Mass Transfer 12 (1969) 187–198.
[15] J.-M. Delhaye, R. Semeria, J.-C. Flamand, Void fraction and vapor and liquid temperatures: Local measurements in two-phase flow using a microthermocouple, J. Heat Transfer 95 (1973) 365–370.
[16] E.N. Ganic, N.H. Afgan, An analysis of temperature fields in the bubble and liquid environment in pool boiling of water, Int. J. Heat Mass Transfer 18 (1975) 301–310.
[17] P. Beckman, R.P. Roy, K. Whitfield, A. Hasan, A fast-response microthermocouple, Rev. Sci. Instrum. 64 (1993) 2947–2951.

[18] P. Beckman, R.P. Roy, V. Velidandia, M. Capizzani, An improved fast-response microthermocouple, Rev. Sci. Instrum. 66 (1995).
[19] J.-M. Delhaye, R. Semeria, J.-C. Flamand, Mesure du taux de vide local et des temperatures du liquide et de la vapeur en ecoulement diphasique avec changement de phase a l'aide d'un microthermocouple, Technical Report CEA-R-4302, November 1972.
[20] A.H. Howard, I. Mudawar, Orientation effects on pool boiling critical heat flux (chf) and modeling of chf for near vertical surfaces, Int. J. Heat Mass Transfer 42 (1999) 1665–1688.
[21] D. Gorenflo, VLE measurements of thoroughly degassed FC-3284, Private communication, 2003.
[22] 3M Company, Specialty Materials Europe Division, Brochure: "The Nature of Fluorinert^{TM} Electronic Liquids", 2003.
[23] P. Skritek, Handbuch der Audio Schaltungstechnik, Franzis, München, 1988.
[24] T. Lüttich, W. Marquardt, M. Buchholz, H. Auracher, Identification of unifying heat transfer mechanisms along the entire boiling curve, Int. J. Therm. Sci. 45 (3) (2006) 284–298 (this issue).
[25] P. Stephan, J. Hammer, A new model for nucleate boiling heat transfer, Wärme- und Stoffübertragung 30 (1994) 119–125.
[26] S.G. Kandlikar, M. Shoji, V.J. Dhir, Handbook of Phase Change, Taylor and Francis, London, 1999.